FEBS 29753 FEBS Letters 579 (2005) 4165–4174

Arabidopsis thaliana MTP1 is a Zn transporter in the vacuolar membrane which mediates Zn detoxification and drives leaf Zn accumulation

Anne-Garlonn Desbrosses-Fonrouge[a,1], Katrin Voigt[a,1,2], Astrid Schröder[a,3], Stéphanie Arrivault[a], Sébastien Thomine[b], Ute Krämer[a,*]

[a] *Max Planck Institute of Molecular Plant Physiology, Am Mühlenberg 1, D-14476 Golm, Germany*
[b] *Institut des Sciences du Végétal, C.N.R.S., Avenue de la Terrasse, 91198 Gif-sur-Yvette Cedex, France*

Received 21 April 2005; revised 21 June 2005; accepted 22 June 2005

Available online 6 July 2005

Edited by Julian Schroeder

Abstract **The *Arabidopsis thaliana* metal tolerance protein 1 (MTP1) of the cation diffusion facilitator family of membrane transport proteins can mediate the detoxification of Zn in Arabidopsis and yeast. *Xenopus laevis* oocytes expressing AtMTP1 accumulate more Zn than oocytes expressing the $AtMTP1_{D94A}$ mutant or water-injected oocytes. An AtMTP1-GFP fusion protein localizes to the vacuolar membrane in root and leaf cells. The analysis of Arabidopsis transformed with a promoter-GUS construct suggests that AtMTP1 is not produced throughout the plant, but primarily in the subpopulation of dividing, differentiating and expanding cells. RNA interference-mediated silencing of *AtMTP1* causes Zn hypersensitivity and a reduction in Zn concentrations in vegetative plant tissues.**

Keywords: Cation efflux; Intron-spliced hairpin; ZAT; Zinc; Metal tolerance; Hyperaccumulation

1. Introduction

All organisms require small amounts of the micronutrient metal ion Zn^{2+}, which acts as a metallic cofactor in a large number of zinc metalloproteins. Zinc-dependent proteins include, for example, Zn finger-containing transcription factors and more than 400 enzymes, for example Cu/Zn superoxide dismutase, carbonic anhydrase, and Zn-metalloproteases [1,2]. Nutritional zinc deficiency is now thought to affect 20% of the World's population and can impair, for instance, the performance of the immune system, as well as growth and neurobehavioural development in children [3]. In the human monogenic autosomal disease *Acrodermatitis enteropathica*, which is associated with severe Zn deficiency symptoms such as skin lesions, a genetic defect in the human Zn transporter gene *hZIP4* interferes with Zn absorption in the intestine [4,5]. Despite their essentiality, Zn^{2+} ions can cause toxicity when accumulated in excess. In plants, an excess of zinc leads to the inhibition of root growth, decreased photosynthetic rates and chlorosis [6]. All organisms have to control very tightly the uptake, speciation and localization of Zn and other metals.

Plasma membrane Zn uptake systems are of key importance for the control of metal entry into cells. In the yeast *Saccharomyces cerevisiae*, in the plant *Arabidopsis thaliana* and in humans, the major known cellular Zn uptake systems are members of the ZIP (*z*inc-regulated transporter, *i*ron-regulated transporter *p*rotein) family [7–10]. The expression of a number of ZIP genes from yeast, humans and plants is upregulated under Zn deficiency and downregulated under Zn sufficient conditions. In addition, in yeast and humans, ZIP proteins are removed from the plasma membrane post-translationally when cells are moved from Zn-deficient to sufficient conditions, thereby inactivating Zn uptake [11–13]. However, merely controlling cellular Zn uptake is not sufficient. When Zn-deficient yeast cells are transferred to media containing high concentrations of zinc, cellular zinc influx rates through ScZrt1p and ScZrt2p are very high before the removal of the transporters from the plasma membrane is completed [14]. This condition has been referred to as "zinc shock", and it requires the operation of highly effective intracellular detoxification mechanisms.

Two transport proteins in the vacuolar membrane, ScZrc1p and ScCot1p, are important for Zn detoxification in yeast cells under conditions of "zinc shock" and during exposure to high Zn concentrations [15–17]. These transporters belong to the ubiquitous cation diffusion facilitator (CDF) family of proteins [18], and have been shown to mediate the transport of Zn^{2+} into the vacuole. The Zrc1p-mediated transport of Zn^{2+} into vacuole-enriched microsomal vesicles is dependent on ATP and requires an inside-acidic proton gradient [19]. ScZrc1p, the *Escherichia coli* CDF protein ZitB and the *Bacillus subtilis* CDF protein CzcD [20,21] have been proposed to operate as Zn^{2+}-proton antiporters. Proteins of the CDF family generally mediate the efflux of metal ions from the cytoplasm [22,23]. The genome of

*Corresponding author. Fax: +49 (0) 331 5678 408.
E-mail address: kraemer@mpimp.golm.mpg.de (U. Krämer).

[1] These authors contributed equally to the manuscript.
[2] Present address: Max-Delbrück-Zentrum für Molekulare Medizin, Robert Rössle Str. 10, 13092 Berlin, Germany.
[3] Present address: Bayer BioScience GmbH, Hermannswerder 20a, D-14473 Potsdam, Germany.

Abbreviations: bp, base pairs; cDNA, complementary DNA; Col, *Arabidopsis thaliana* accession Columbia; EGFP, enhanced green fluorescent protein; GFP, green fluorescent protein; HEPES, *N*-2-hydroxyethylpiperazine-*N*′-3-propanesulfonic acid; RT-PCR, reverse transcriptase-polymerase chain reaction; SC, synthetic complete minimal medium; S.D., standard deviation; S.E., standard error of the mean; URA, uracil; Zn, zinc

0014-5793/$30.00
doi:10.1016/j.febslet.2005.06.046

A. thaliana encodes 12 putative proteins which are highly divergent in sequence, but share some characteristics of CDF family membrane transport proteins [24]. These characteristics include six predicted membrane-spanning segments, C- and N-termini predicted to be oriented towards the cytoplasmic side, a large and often histidine-rich cytoplasmic region between predicted transmembrane segments four and five, a signature sequence **S**X-(ASG)(LIVMT)$_2$(SAT)(DA)(SGAL)(LIVFYA)(HDN)X$_3$**D**X$_2$(AS) between the first and second membrane-spanning segment [18,23], and significant sequence conservation within the cation efflux domain which encompasses all transmembrane segments and part of the cytoplasmic C-terminus (http://pfam.wustl.edu/cgi-bin/getdesc?acc=PF01545).

The first plant CDF protein, identified at the complementary DNA (cDNA) level, was ZAT (zinc transporter of *A. thaliana*) and was later renamed AtMTP1 (metal tolerance protein 1) [25,26]. By reverse transcriptase-polymerase chain reaction (RT-PCR), *AtMTP1* transcripts were shown to be present at equally low levels in whole seedlings grown under normal or excess Zn supply [25]. Ectopic overexpression of the *AtMTP1* cDNA under the control of a cauliflower mosaic virus (CaMV) 35S promoter resulted in enhanced Zn tolerance of transgenic seedlings and slightly increased zinc accumulation in the roots. Two out of the 12 putative CDF proteins of *A. thaliana*, AtMTP2 and AtMTP3, are closely related to AtMTP1 (64.4% and 67.6% identity, and 71.2% and 76.1% similarity, respectively).

Homologues of AtMTP1 have been implicated in metal tolerance of metal hyperaccumulator plants, namely the TgMTP1 protein in *Thlaspi goesingense* [27,28] and the AhMTP1 protein in *Arabidopsis halleri* [29]. A further AtMTP1-related protein is poplar PtdMTP1, which, when ectopically expressed in *A. thaliana*, confers enhanced zinc tolerance, analogous to AtMTP1 [24]. All plant MTP1-like proteins described so far have been reported to complement the zinc hypersensitivity of a mutant of *S. cerevisiae* which lacks one or both of the two CDF transporters Zrc1p and Cot1p that can transport Zn^{2+} into the yeast vacuole. Expression of the *Stylosanthes hamata* MTP1 has been reported to confer Mn tolerance to yeast cells [30]. This protein has now been renamed ShMTP8 (AY181256) because it belongs to a distinct group of plant CDF proteins and shares only 25% sequence similarity (10% identity) with AtMTP1. Based on the localization of chimeric green fluorescent protein (GFP) fusion proteins, some plant MTP1-like proteins operate in the vacuolar membrane, as found for PtdMTP1, AhMTP1 and AtMTP1, whereas others are in the plasma membrane, as reported for TgMTP1 [24,28,29,31].

Here we present evidence for the transport of Zn^{2+} by the AtMTP1 protein expressed heterologously in yeast and in *Xenopus laevis* oocytes. Furthermore, we examine the function of AtMTP1 in metal homeostasis of *A. thaliana* by determining the regulation and localization of *MTP1* expression and by investigating Zn partitioning and Zn tolerance in plants transformed with an intron-spliced hairpin construct designed for RNA-interference-mediated silencing of *AtMTP1*.

2. Materials and methods

2.1. Plant material and growth conditions

Seeds of *A. thaliana* (L.) Heynhold (Col) were used throughout (Lehle Seeds, Round Rock, TX, USA). Sterile plant growth was performed in square plastic Petri plates (14 cm) in a climate-controlled growth cabinet (20 °C day/18 °C night; 60% relative humidity day/75% night; 11 h day with illumination at a light intensity of 120 μmol m^{-2} s^{-1}). Plants on soil were cultivated in 1:1 (v/v) standard soil (GS90) and vermiculite in a greenhouse with the following settings: 20 °C day/18 °C night, 50% relative humidity day/80% night, 16 h day, with supplementary lighting provided by mercury vapor lamps to give a total light intensity of approximately 250 μmol m^{-2} s^{-1}. Hydroponic plant culture was performed in a modified 0.25-strength Hoagland solution as described [32] in a climate-controlled growth chamber (temperature: 20 °C day/16 °C night; relative humidity: 60% day/75% night; light: 16 h day/8 h night and a light intensity of 120 μmol m^{-2} s^{-1}). Plants were supported by floating polystyrene lids. After germination, solutions were exchanged weekly.

2.2. Cloning and DNA manipulations

Cloning and DNA manipulations were performed using standard procedures [33] and according to the instructions from manufacturers. A DNA fragment containing the coding sequence of *AtMTP1* (At2g46800) was amplified by PCR from cDNA using the forward primer 5′-CACCATGGAGTCTTCAAGTCCCCACC-3′, and reverse primers 5′-TTAGCGCTCGATTTGTATCGTGAC-3′ (with stop codon) or 5′-GCGCTCGATTTGTATCGTGACATG-3′ (without stop codon), respectively, and Pfu Turbo DNA polymerase (Stratagene, La Jolla, CA, USA), and the following program: 35 cycles of 95 °C for 30 s, 55 °C for 30 s, 72 °C for 2 min. The PCR product was introduced into the entry vector pENTR/D-TOPO (pENTR/D-TOPO cloning kit, Invitrogen, Carlsbad, CA, USA) by site-directed recombination. The mutant *AtMTP1*$_{D94A}$ was generated in pENTR/D-TOPO-*MTP1* using a previously described technique [29], employing primers 5′-GCTCATTTGCTCTCT*GCC*GTTGCTGCCTTTGC-3′ and 5′-GCAAAGGCAGCAACGGCAGAGAGCAAATGAGC-3′ (10 cycles of 95 °C for 30 s, 55 °C for 60 s, 68 °C for 12 min), followed by digestion of the parent DNA with *Dpn*I, which digests methylated and hemimethylated DNA, and subsequent transformation of *E. coli* for repair of the doubly nicked plasmid. All entry clones were verified by sequencing.

2.3. Expression of *AtMTP1* in oocytes of X. laevis

The 1197-bp coding sequence of the *AtMTP1* cDNA was subcloned into a GATEWAY-converted (F.Porée, University of Potsdam) pGEMHE vector [34]. Capped complementary RNA (cRNA) was synthesized in vitro using either the mMESSAGE mMACHINE T7 kit or the mMESSAGE mMACHINE T7 Ultra kit (Ambion, Austin, TX). Stage V and VI Xenopus oocytes were prepared as described previously [35]. For Zn accumulation experiments, oocytes were injected with 50 nL H_2O, or 25 ng cRNA per oocyte for *AtMTP1* or *AtMTP1*$_{D94A}$, respectively. Injected oocytes were maintained in Barth's medium, composed as follows: 10 mM *N*-2-hydroxyethylpiperazine-*N*′-3-propanesulfonic acid (HEPES)–NaOH pH 7.4, 88 mM NaCl, 1 mM KCl, 2.4 mM $NaHCO_3$, 0.33 mM $Ca(NO_3)_2$, 0.41 mM $CaCl_2$, 0.82 mM $MgSO_4$, supplemented with 10 mg L^{-1} gentamycin. Seventy-two hours after injection, pools of 50 oocytes were subjected to the following treatments at 25 °C: 30 min in OR2 medium or 30 min in OR2 medium supplemented with 0.1 mM $ZnSO_4$, respectively. The OR2 medium was composed as follows: 82.5 mM NaCl, 2 mM KCl, 1 mM $MgCl_2$, and 5 mM HEPES; pH was adjusted to 7.4 with NaOH. After the exposures, oocyte pools were transferred onto ice immediately and rinsed three times with ice-cold OR2 medium at pH 8.5. Subsequently, the remaining drops of medium were carefully removed. Oocytes were dried at 60 °C for 3 days. Oocyte pools were digested and analyzed as described [32] by inductively-coupled plasma optical emission spectrometry (ICP-OES). The experiment was repeated independently using a different batch of oocytes. Results were qualitatively similar, but all oocytes contained higher Zn concentrations.

2.4. Expression of *AtMTP1* in the yeast S. cerevisiae

To generate yeast expression constructs, the *AtMTP1* cDNAs were introduced into the target vector pFL613 [29], which generates a translational fusion of the encoded protein to an N-terminal triple hemagglutinin (3 × HA) epitope tag. Transformation of the *zcr1 cot1* double mutant strain was performed as described [29], and transformants were selected on synthetic complete minimal medium (SC)-URA. For each construct, overnight liquid cultures of four independent transformant colonies grown in low phosphate low sulphate synthetic minimal

medium (LSP)-URA medium supplemented with 2% (w/v) glucose and 1.4 μM $ZnSO_4$, were washed once in fresh culture medium and used to inoculate 4 mL of the same medium with concentrations of added $ZnSO_4$ between 50 μM and 2 mM, at a cell density of 10^5 cells mL^{-1}. Cultures were incubated at 30 °C with constant mixing in a culture wheel. Optical density was measured at 600 nm in 5- to 8-h intervals. The doubling time was determined for the phase of maximum growth between 19 and 24 h after the beginning of cultivation. The experiment was repeated three times. Cells were collected by centrifugation from low Zn control cultures of equivalent cell densities after 48 h of culture. Total protein was extracted, separated on a 10% (v/v) denaturing sodium dodecyl sulfate–polyacrylamide gel [36], and blotted [37] onto a PVDF membrane (Immobilon™, Bedford, MA, USA) using a semi-dry blotting apparatus (Fastblot B33, Biometra GmbH, Göttingen, Germany). Membranes were blocked in 10% (w/v) milk powder, 0.1% (v/v) Tween 20 in tris-hydroxymethyl aminomethane-buffered saline (TBS), and then incubated in a solution of 1% (w/v) milk powder, 0.125% (v/v) Tween 20 in TBS containing 1:5000 monoclonal mouse anti-HA antibody (Covance Research Products, Santa Clara, CA, USA). Membranes were washed three times in the same solution without antibodies for 10 min, and then incubated in the same solution containing 1:10 000 anti-mouse-Igg coupled to horseradish peroxidase (Amersham Biosciences, Little Chalfont, UK) for 4 h, followed by three washes as described above, and chemiluminescent detection (ECL kit; Amersham Biosciences, Little Chalfont, UK).

For neutral red loading, 4-mL cultures of equivalent cell densities grown in minimal medium at 1.4 μM Zn for 56 h were sedimented at $1000 \times g$ for 5 min, resuspended in an equal volume of fresh minimal medium and incubated with mixing at 30 °C for 45 min. After sedimentation, yeast cells were suspended in 4 mL 100 mM Na_2CO_3, at pH 9.4 adjusted with HCl, containing 0.04% (w/v) neutral red and incubated at 30 °C with gentle agitation for 10 min. Cells were washed once in 4 mL 50 mM potassium phosphate buffer at pH 7.5, and finally suspended in 100 μL of the same buffer. Equal volumes (50 μL) were transferred into each well of a 96-well microtiter plate for scanning of the color image.

2.5. Expression of GFP fusion proteins and confocal microscopy

To generate a construct encoding a chimeric fusion protein of an N-terminal RSsm-GFP [38,39] and AtMTP1, the *AtMTP1* cDNA was subcloned by in vitro site-directed recombination (Invitrogen) into the plant transient expression vector pA7-p35S-N-GFP (Katrin Czempinsky, University of Potsdam, Germany), adapted for Gateway cloning (Ben Trevaskis, CSIRO Plant Industry, Canberra, Australia). Protoplasts were prepared from an *A. thaliana* suspension culture and transfected, as described [29]. Between 24 and 48 h after transfection fluorescence was imaged by confocal microscopy (Leica TCS SP2, Leica Microsystem, Wetzlar, Germany) with excitation at 488 nm, and the GFP fluorescence emission signal was detected between 505 and 520 nm. A coding sequence of the *AtMTP1* cDNA lacking the translational stop codon was introduced by site-directed recombination into the binary vector pK7FWG2 [40], designed for translational fusion of the encoded protein to a C-terminal enhanced green fluorescent protein (EGFP). The resulting vector was introduced into *Agrobacterium tumefaciens* by electroporation, and six *A. thaliana* (Col) plants were used for transformation employing the floral dip method [41]. Transformant individuals were selected on vertical plates containing 0.5× Murashige & Skoog (MS) medium, 0.5% (w/v) sucrose, 0.8% (w/v) phytagar (Invitrogen) and 50 mg L^{-1} kanamycin (Duchefa, Haarlem, The Netherlands) for 6–13 days. Seedlings were incubated in a solution of 1 mg mL^{-1} propidium iodide (Molecular Probes, Inc., Eugene, OR) in ultrapure water for 0.5 h before observation. Transformants were analyzed in the T2 generation, and the images shown are representative of a total of four analyzed independent transgenic lines.

2.6. Quantitative real-time RT-PCR analysis of AtMTP1 expression in *wild-type* A. thaliana

Two plants were grown hydroponically in 400 mL nutrient solution in each culture vessel as described above. Plant organs were harvested from six-week-old flowering plants, generating pooled samples from four plants grown in two replicate culture vessels per sample. Organs were sampled as follows: opened flowers, the five oldest green siliques, all cauline leaves, a 2-cm section of the inflorescence stem at mid-height, the entire root system without the hypocotyls, and rosette leaves from an intermediate position within the rosette. All plant tissues were frozen immediately in liquid nitrogen and subsequently stored at 80 °C. Total RNA was isolated from 100 mg subsamples after homogenization using RNeasy Plant Mini Kit (Qiagen, Hilden, Germany). The quantity of RNA was determined spectrophotometrically, and its quality was checked by agarose gel electrophoresis. RNA was treated with RNase-free DNase-I (Ambion) for 30 min followed by DNase-I removal. Two micrograms of DNA-free RNA was reverse transcribed using First-Stand Synthesis System for RT-PCR (Invitrogen) according to the manufacturer's specifications. The absence of genomic DNA was verified by performing a control reaction omitting reverse transcriptase for each template, and by performing PCR with primers for the *AtAKT1* gene (At2g26650), 5′-ATCGGATAACAATGGCAGAACAC-3′ and 5′-GCAGGACGG-ATGTTGGGTTCACTA-3′. These primers span an intron of the genomic *AtAKT1* sequence, and thus amplify a product of 579 bp from cDNA, and 766 bp from genomic DNA. PCR conditions and primers were optimized for amplification efficiencies of 100 ± 5% for all primer pairs used. *AtMTP1*-specific primers were 5′-ACGGCCATGACCAT-CACAATC-3′ and 5′-TGCTTGTCCTCTCCATGACCA-3′. Primers specific for the constitutively expressed control gene *AtCYP5* (cyclophilin; At2g29960) were 5′-CCAGGTGTACTTTCAATGGCG-3′ and 5′-CAAACACCACATGCCTTCCA-3′. These primer pairs were designed to specifically amplify fragments of approximately 120 bp of the coding sequence (Primer Express version 2.0, Applied Biosystems, Foster City, CA, USA). The real-time PCR was performed using the qPCR MasterMix for SYBR green kit (RT-SN2X-03, Eurogentec, Seraing, Begium), in a total volume of 25 μL, including 0.1–10 ng of cDNA, and gene-specific primers (250 nM final concentration). Amplification of PCR products was monitored via intercalation of SYBR Green using an ABI PRISM 5700 or 7900HT sequence detection system (Applied Biosystems, Foster city, California, USA). Amplification was performed for 40 cycles, and data were analyzed as described [32]. Amplification efficiency was calculated using absolute fluorescence data captured during the exponential phase of amplification of each real-time PCR [42,43] to ensure equal amplification for all primer pairs. The relative transcript level for *AtMTP1* was calculated by normalizing to *AtCYP5* as follows: $RTL = 2^{-\Delta C_T}$, whereby $\Delta C_T = C_T(MTP1) - C_T(CYP5)$. After completion of each PCR reaction, all PCR products were checked by melting-curve analysis and by agarose gel electrophoresis. Three independent replicate experiments were conducted.

2.7. GUS activity staining and microscopy

The generation of a fusion construct of the promoter region of *AtMTP1* and the *E. coli uidA* gene was out-contracted (Hermann Schmidt, DNA Cloning Service, Hamburg, Germany). The constructs were made from PCR products amplified from *A. thaliana* (Col) genomic DNA, in the vector pGPTV-Kan [44]. Based on full-length *AtMTP1* cDNAs available in the databases (http://signal.salk.edu/cgi-bin/tdnaexpress), the construct incorporated 1537 bp of the promoter region, followed by the genomic region encoding the 5′-UTR of *AtMTP1* and containing one or two introns upstream of the intron-less coding sequence of *AtMTP1*, as well as the first 357 bp of the *AtMTP1* coding sequence. Constructs were verified by sequencing and sequentially introduced into *A. tumefaciens* and *A. thaliana* as described above. Histochemical staining was performed in the T2 generation, using eleven independent transgenic lines for seedlings and seven independent lines for flowers and siliques. Seeds were surface-sterilized and germinated on 0.5× Murashige & Skoog medium containing 0.5% (w/v) sucrose and 50 mg L^{-1} kanamycin. Plant tissues were harvested as indicated and immediately transferred into ice-cold 90% (v/v) acetone, and subsequently incubated at room temperature for 20 min. Tissues were washed in staining buffer (0.2% (v/v) Triton X-100; 50 mM Na-PO_4 buffer, pH 7.2; 2 mM potassium ferrocyanide; 2 mM potassium ferricyanide), and subsequently transferred into staining buffer supplemented with 2 mM Cyclohexylammonium 5-bromo-4-chloro-3-indolyl-β-D-glucuronate (X-Gluc, Duchefa). Samples were infiltrated under vacuum for 20 min and stained at 37 °C for 4 h. After successive incubation in 20%, 35%, and 50% (v/v) ethanol, each for 30 min, samples were placed in fixative (50% (v/v) ethanol; 5% (v/v) formaldehyde; 10% (v/v) acetic acid) for 30 min. Samples were kept in 90% (v/v) ethanol at 4 °C or room temperature. Selected tissues were embedded in Technovit (Technovit 7100 and 3040, Heraeus Kulzer, Hanau, Germany) resin for subsequent sectioning using a

microtome (RM 2155, Leica, Wetzlar, Germany). Other samples were embedded in 5% (w/v) low melt agarose in ddH_2O and cut using a vibratome (VT 1000 S, Leica). Sections of 275 μm thickness were stained in a solution contained 100 mM Na-PO_4 buffer (pH 7.2), 10 mM EDTA, 3 mM potassium ferrocyanide, 0.1% (v/v) Triton X-100 and 2 mM X-Gluc, as described above.

2.8. Generation and analysis of A. thaliana transformed with an AtMTP1 RNA interference construct

A 600-bp fragment encompassing nucleotides 152–752 of the 1197-bp-long coding sequence of *AtMTP1* was amplified from cDNA using primers 5′-TATCTAGAGGCGCGCCGCTCTGCTTCTATGCGGA-3′ and 5′-ACGGATCCATTTAAATTCTTTTGCTGCGACTTGA-3′. The restriction sites introduced by the primers, *Asc*I and *Swa*I, and *Bam*HI and *Xba*I, respectively, were used to sequentially introduce the fragment in opposite orientation into the binary vector pFGC5941 (ChromDB; http://www.chromdb.org/index.html, chromdb@ag.arizona.edu, University of Arizona, AR, USA). After transformation of *A. thaliana* (Col) as described above, seeds of the T1 generation were surface-sterilized, and transformants were selected on vertical plates filled with 0.5× Murashige & Skoog (MS) medium containing 0.5% (w/v) sucrose, 0.025 mg ml^{-1} DL-phosphinotricine (Duchefa) and 0.8% (w/v) phytagar (Invitrogen). Each selected individual plant thus represented an independent transformant line. For experiments, 10-day-old seedlings were transferred either onto soil, or onto vertical plastic Petri dishes containing modified 0.25-strength Hoagland solution [32] with 0.5% (w/v) sucrose, 0.8% (w/v) phytagar and between 1 μM and 200 μM $ZnSO_4$. Three replicate plates, each containing ten seedlings, were set up for each genotype and each Zn concentration. Plants were photographed and harvested after 7 days for the determination of final root length and the analysis of transcript levels. RNA was extracted from 4 pooled seedlings grown at 1 μM $ZnSO_4$. Real-time RT-PCR and data analysis were performed as described [32], using the following primers: *AtMTP1*, 5′-TCAGACCAGAAGCAGATGCAGA-3′ and 5′-CTCCCTGCGGATGTAATCAATT-3′; *AtMTP2*, 5′-GGACAACCATTAAGATGCTTCG-3′ and 5′-TCTCTCGGTGTGCTCTCCATTA-3′; *AtMTP3*, 5′-GCGATTACTGTCGGCAAACTTT-3′ and 5′-AAACCATATCTGCCTCTGCCTC-3′. Three independent replicate experiments were performed for the analysis of transcript levels and Zn tolerance. For the determination of Zn accumulation, 17-day-old plants were transferred individually into 6 cm pots of soil following selection as described above. After growth in the greenhouse for 27 days, plant tissues were harvested separately. Seeds were harvested at maturity. Tissues collected from nine replicate plants were pooled from groups of three plants to generate three independent replicate samples. Plant tissues were washed in deionized water, blotted on tissue paper, dried and analyzed by inductively-coupled optical emission spectrometry as described [32]. Data shown are representative of three independent biological experiments.

3. Results

3.1. Comparative Analysis of AtMTP1 and $AtMTP1_{D94A}$ by heterologous expression in yeast cells and in oocytes

In order to address the transport function of AtMTP1, the AtMTP1 protein or the $AtMTP1_{D94A}$ mutant protein were expressed in yeast. In the $AtMTP1_{D94A}$ protein, an aspartate residue, which is strictly conserved in all members of the CDF protein family [23] and located in the second predicted membrane-spanning segment within the CDF signature sequence, was replaced by an alanine. An analogous mutation of the corresponding residue in the *A. halleri* MTP1 protein results in the loss of the ability to complement the zinc sensitive *zrc1 cot1* double mutant of *S. cerevisiae* [15,29]. As shown before [29], the expression of AtMTP1 complemented the Zn sensitivity of the *zrc1 cot1* double mutant (Fig. 1A). In addition, including several low Zn concentrations revealed that the expression of $AtMTP1_{D94A}$ exacerbated Zn hypersensitivity of the double mutant (Fig. 1A). Both proteins were expressed in yeast cells in comparable amounts (Fig. 1B). This

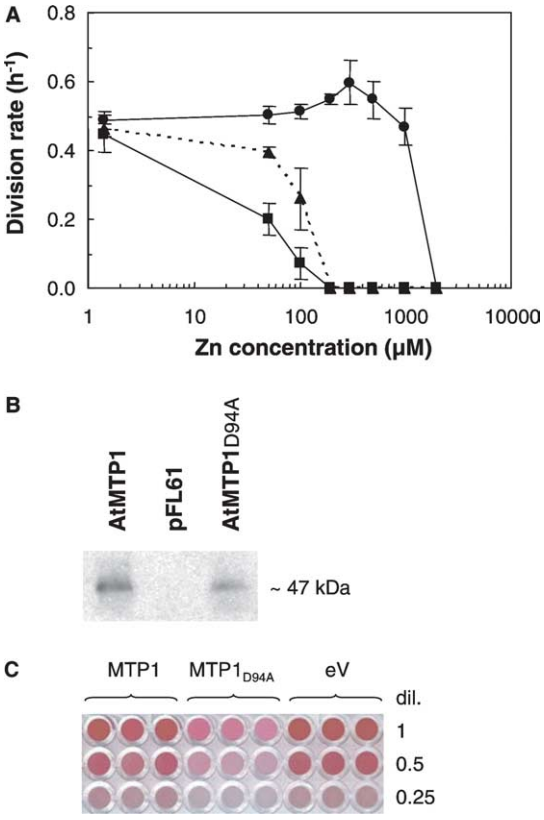

Fig. 1. Expression of AtMTP1 complements, and expression of $AtMTP1_{D94A}$ exacerbates, zinc sensitivity of the *zrc1 cot1* mutant of *S. cerevisiae*. (A) Zinc tolerance in liquid culture. Shown are the numbers of cell divisions per hour during the logarithmic growth phase, as a function of the zinc concentration in the medium. Values are arithmetic means ± S.D. of $n = 4$ independent transformants of the *zrc1 cot1* mutant strain expressing (–●–) 3HA-AtMTP1, (–■–) 3HA-$AtMTP1_{D94A}$. Data for the *zrc1 cot1* mutant transformed with the (...▲...) empty pFL61 vector are also shown. Liquid minimal medium was supplemented with $ZnSO_4$ as indicated in the diagram and inoculated with yeast cells at an initial cell density of 10^5 cells mL^{-1}. The OD_{600} values measured at 19 and 24 h after inoculation were used to calculate doubling times. Data shown are from one experiment representative of a total of three independent experiments. (B) Signals on a Western blot of total protein extracts from the transformants described in (A), after incubation with an anti-HA antibody. Data shown are from one experiment representative of a total of two independent experiments. (C) Yeast cells expressing $AtMTP1_{D94A}$ accumulate less neutral red than cells expressing AtMTP1 or yeast cells transformed with an empty vector. Yeast cultures of equivalent cell densities were equilibrated in an alkaline sodium carbonate solution containing 0.04% (w/v) neutral red for 10 min, and then washed. For each construct, three dilutions are shown for each of three independent yeast transformants. The image shown is from one experiment representative of a total of two independent experiments. dil., dilution factor.

suggested that $AtMTP1_{D94A}$ was not only unable to mediate the detoxification of Zn^{2+} in the yeast vacuole, but caused additional stress. To gain more information, we allowed cells to equilibrate in a neutral red solution at alkaline pH, a condition which should allow passive diffusion of the uncharged neutral red molecule, a weak base, and trapping in acidic compartments upon protonation. The less intense red staining of $AtMTP1_{D94A}$ -expressing yeast cells, when compared with AtMTP1-expressing cells or empty vector transformants, suggests that $AtMTP1_{D94A}$ expression results in a reduced ability

Table 1
Zn accumulation in *X. laevis* oocytes expressing AtMTP1 or $AtMTP1_{D94A}$

cRNA	Zn concentration	
Zn	0 Zn	0.1 mM
	nmol per oocyte	
AtMTP1	1.17	1.25
$AtMTP1_{D94A}$	1.37	1.01
Control (water)	1.36	1.02

Pools of 50 oocytes were incubated in OR2 medium (pH 7.4), with or without 0.1 mM added $ZnSO_4$ for 30 min.
Zn concentrations were determined by ICP-OES. The data are from one experiment representative of two independent experiments performed using different batches of oocytes.

of yeast cells to maintain an acidic vacuolar lumen (Fig. 1C). This observation may be due to the leakage of protons through the mutant transporter. Alternatively, another ion, such as Na^+, may leak through the transporter and lead indirectly to a depletion of the proton gradient.

Next we tested whether Zn accumulation in oocytes injected with *MTP1* cRNA differed from Zn accumulation in oocytes injected with $MTP1_{D94A}$ cRNA or with water. Oocytes injected with *MTP1* cRNA contained on average 1.17 nmol Zn per oocyte after incubation in control medium and 1.25 nmol Zn per oocyte after exposure to the Zn-supplemented medium (Table 1). This suggests a net influx of 0.08 nmol Zn per oocyte during exposure to 0.1 mM $ZnSO_4$ for 30 min. In water-injected and $AtMTP1_{D94A}$-injected oocytes mean Zn concentrations were very similar and amounted to between 1.35 and 1.36 nmol Zn per oocyte for control (no added Zn) oocytes and between 1.01 and 1.02 nmol Zn per oocyte in Zn-exposed oocytes (Table 1). This suggests a net efflux of approximately 0.34 nmol Zn per oocyte in control oocytes during exposure to 0.1 mM Zn for 30 min. The apparent net Zn efflux in water or $AtMTP1_{D94A}$-injected oocytes upon exposure to Zn is likely to reflect the induction of an endogenous Zn export activity during exposure to Zn for 30 min. Most probably, this export activity was also present in *AtMTP1*-injected oocytes. The correction for MTP1-independent Zn efflux thus results in a total MTP1-dependent Zn influx of 0.42 nmol per oocyte in 30 min. [4] These data are consistent with a significant proportion of the MTP1 protein localizing to the plasma membrane of oocytes in this expression system and mediating the cellular influx of Zn^{2+}. Overall Zn concentrations measured in the oocytes were consistent with the previously reported Zn content of 70 ng (1.08 nmol) per oocyte in stage VI [45].

3.2. Subcellular localization of the AtMTP1 protein

To determine the subcellular localization of AtMTP1 we localized a transiently expressed fusion protein of an N-terminal GFP moiety and AtMTP1, in protoplasts of *A. thaliana* (Fig. 2A). GFP fluorescence was localized to the vacuolar membrane of transfected protoplasts. To verify these results we generated stable *A. thaliana* transformants expressing AtMTP1 with an EGFP moiety fused to its C-terminus. The GFP fluorescence signal was localized to the vacuolar membrane in leaf as well as root cells (Fig. 2B and C, respectively). These results suggest that AtMTP1 localizes to the vacuolar membrane of plant cells. Two attempts of generating an AtMTP1-specific antibody were unsuccessful.

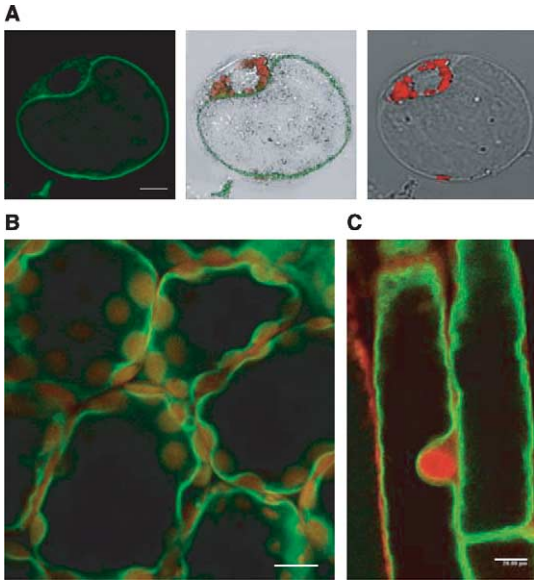

Fig. 2. A chimeric fusion protein of AtMTP1 and GFP localizes to the vacuolar membrane of *Arabidopsis* cells. (A) GFP fluorescence image of GFP-AtMTP1 (left), overlay of GFP fluorescence, transmission and chlorophyll fluorescence images (middle), and overlay of transmission and chlorophyll fluorescence images (right) of an *A. thaliana* protoplast 24 h after transfection. The size bar corresponds to 8 μm. Images are from one transfected protoplast representative of a total of at least ten. (B) Fluorescence image of a leaf epidermis of a transgenic seedling of *A. thaliana* expressing AtMTP1-GFP. Chlorophyll and propidium iodide fluorescence are shown in red, and the GFP signal in green. The size bar corresponds to 4 μm. (C) Fluorescence image of root epidermal cells of a transgenic seedling of *A. thaliana* expressing AtMTP1-GFP. The propidium iodide signal is shown in red, and the GFP signal in green. The size bar corresponds to 20 μm. Images in (B) and (C) are from one transformant line (T2 generation) representative of four independent lines. Seedlings were stained with propidium iodide to visualize cell walls and nuclear DNA.

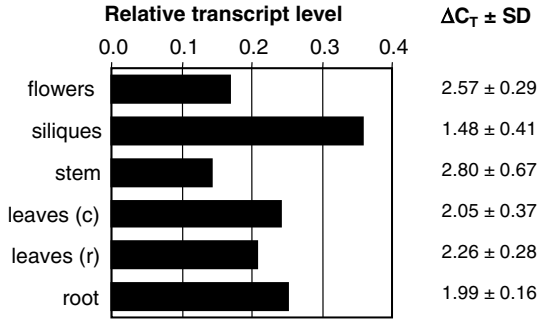

Fig. 3. *AtMTP1* transcripts are present in all plant organs. Transcript levels were determined in different organs of hydroponically cultivated six-week-old flowering *A. thaliana* plants by quantitative real-time RT-PCR. Values are mean ΔC_T ± S.D. (right) and mean relative transcript levels (left) calculated from two technical replicates from one experiment representative of a total of three independent biological experiments. The ΔC_T values were calculated as follows: $\Delta C_T = C_T(AtMTP1) - C_T$ (constitutive control gene: *AtCYP5*). Relative transcript levels were calculated as follows: $RTL = 2^{-\Delta CT}$.

[4] Zn uptake rates could not be determined using shorter exposures because of the limited sensitivity of ICP-OES. It was also not possible to obtain permission to use the radioisotope ^{65}Zn.

3.3. Transcript analysis and promoter activity

To better understand the in planta function of AtMTP1 we analyzed steady-state *MTP1* transcript levels by real-time RT-PCR. As reported earlier [29], no induction of *AtMTP1* transcripts was observed in response to exposure to Zn in either roots or shoots after exposure for between 2 h and 4 days (data not shown). In addition, we did not observe an increase in transcript levels in either roots or shoots upon exposure to an excess of Cd, Co, Cu, Fe or Mn for 2 days, using quantitative real-time RT-PCR (data not shown). Next we investigated whether *AtMTP1* is expressed differentially in different plant organs (Fig. 3). *AtMTP1* transcripts were detected at similar levels in all analyzed tissues, namely entire mature flowers, the inflorescence stem, cauline and young rosette leaves, as well as in roots of mature plants. In siliques transcript levels were slightly higher than in the other tissues analyzed (Fig. 3).

To gain further information on the expression of *AtMTP1* we analyzed plants transformed with a *GUS* reporter gene construct incorporating approximately 1.5 kpb of the *AtMTP1* promoter region, the 5′ untranslated region of *AtMTP1* containing one or two introns and the first 357 bp of the intron-free *AtMTP1* coding sequence. The construct thus encoded the first two N-terminal transmembrane segments of MTP1, fused to the β-glucuronidase reporter protein. GUS activity was detectable in the youngest leaves of young seedlings (Fig. 4A), as well as in the hydathodes of older leaves. GUS activity was particularly high in the root systems of young 14-day-old seedlings (Fig. 4B). With increasing seedling age, GUS activity decreased in most parts of the roots (data not shown), but remained very high in the tips of main and lateral roots (Fig. 4C and D). In mature plants, there was virtually no histochemically detectable GUS activity in fully expanded leaves (not shown). Flower buds displayed an intense GUS staining, primarily in the carpels (Fig. 4E). GUS activity in carpels decreased during flower maturation and was low and confined to the abscission zone in young siliques (Fig. 4F), but remained high in filaments and in pollen grains of mature flowers (Fig. 4G). GUS activity was also high in the upper part of the inflorescence stem (Fig. 4G), but not detectable in the lower part (not shown). During maturation of siliques GUS activity was highest in developing seeds between 4 and 7 days after pollination, and decreased afterwards (9 and 11 days after pollination, Fig. 4H). In a section of a developing seed, GUS activity was localized in the embryo and endosperm (Fig. 4I).

To investigate whether GUS activity was representative of steady-state transcript levels we analyzed the AtGenExpress data of organs at comparable developmental stages (http://www.arabidopsis.org/info/expression/ATGenExpress.jsp). According to the AtGenExpress data *MTP1* transcript levels are highest in developing seeds and in mature pollen (Fig. 4K). The AtGenExpress database further indicates that in

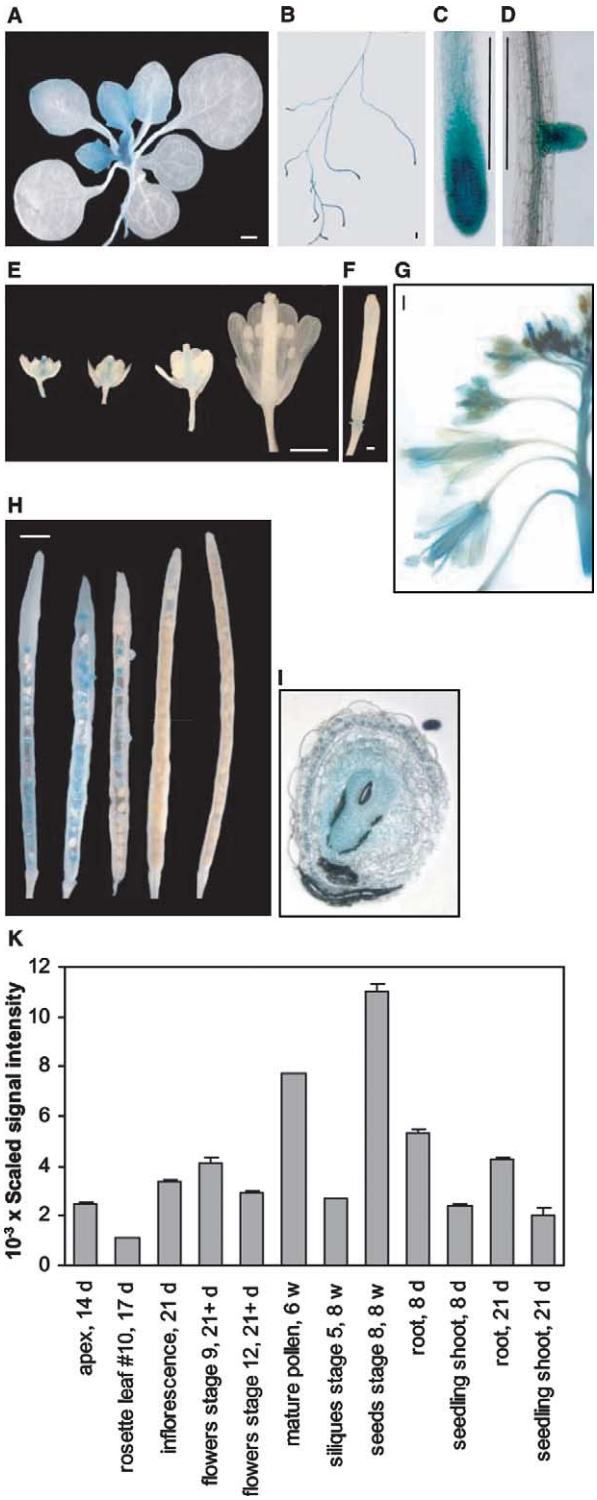

Fig. 4. Localization and developmental regulation of *AtMTP1* promoter activity. (A–I) Histochemical staining for β-glucuronidase activity in *A. thaliana* (Col) lines transformed with a *pAtMTP1::GUS* construct. (A) Shoot of a 20-day-old seedling. (B) Root system of a 14-day-old seedling. (C) Root tip of a 20-day-old seedling. (D) Emerging lateral root tip of a 20-day-old seedling. (E) Flower buds and flowers of a 45-day-old plant. (F) Silique of a 45-day-old plant stained with flowers shown in E. (G) Inflorescence of a 45-day-old plant as used in (E) and (F). (H) Siliques 4, 5, 7, 9 and 11 days (left to right) after pollination. (I) Section of a developing seed containing embryo at torpedo stage 7 days after pollination. Transgenic seedlings of the T2 generation were germinated and grown on 0.5× MS medium on vertical agarose plates for up to 20 days and harvested (A–D), or transferred onto soil (E–I). The shown GUS staining patterns are representative of a total of eleven independent transgenic lines for seedlings, and seven independent lines for flowers and siliques. Scale bars correspond to 1 mm. (K) Relative *AtMTP1* transcript abundance in selected organs and developmental stages. Bars represent arithmetic mean ± S.D. of scaled signal intensities (target value 1000) of a subset from the AtGenExpress data for *AtMTP1* taken from the Genevestigator website (https://www.genevestigator.ethz.ch/~w3pb/genevestigator/index.php?page=home).

young seedlings *AtMTP1* transcript levels are higher in roots than in shoots, and tend to decrease between 8 and 21 days of plant age. Finally, transcript levels are higher in the vegetative apex, the inflorescence and in young flowers than in rosette leaves. The publicly available transcript data is thus qualitatively in agreement with GUS staining patterns in *pAtMTP1::GUS* lines.

3.5. Suppression of AtMTP1 transcript levels by RNA interference

Ectopic overexpression of an *AtMTP1* cDNA under the control of a CaMV 35S promoter has previously been shown to slightly enhance Zn tolerance [25]. This is consistent with the localization of AtMTP1 in the vacuolar membrane and a cellular function in the transport of Zn^{2+} ions into the vacuole for sequestration, as described here. However, in order to define the role of AtMTP1 in planta, a loss-of function mutant is more appropriate. A putative T-DNA knockout line was identified in the Syngenta collection (Garlic_305_A09.b.1a.lb3Fb). This line harbored two tandem T-DNAs in an intron of the *MTP1* gene 306 bp upstream of the translational start codon of *MTP1* (not shown). In this line *MTP1* transcript levels were not reduced compared to wild-type plants (not shown).

A. thaliana plants were transformed with an intron-spliced hairpin construct designed for *MTP1* silencing by RNA interference (RNAi) [46]. This construct contained two identical 600-bp fragments of the *AtMTP1* coding sequence in reverse orientation, separated by an intron, downstream of the strong constitutive CaMV 35S promoter. Based on the assumption that plants with reduced MTP1 protein levels are likely to be zinc-hypersensitive, T1 seeds were selected for expression of the resistance marker, and transformants were subsequently transferred onto media containing high Zn concentrations. All *MTP1*-RNAi transformant individuals were hypersensitive to Zn in the T1 generation (Fig. 5A).

To confirm that *MTP1* transcript levels were reduced in these plants we performed quantitative real-time RT-PCR. On average, transcript levels of *AtMTP1*-RNAi transformant seedlings were reduced to 28.5% of those found in empty vector control transformants in the T1 generation (Fig. 5B). In *A. thaliana* the *MTP2* and *MTP3* coding sequences are the most homologous to *MTP1*, with 65.1% and 62.8% identity, respectively, within the cDNA fragment chosen for RNA interference. The longest stretch of identical nucleotides of 18 consecutive nucleotides is found between the chosen fragment from *MTP1* and the *MTP2* sequence. Relative to empty vector controls, *MTP3* transcript levels were slightly reduced to on average about 83.4%, whereas *MTP2* transcript levels were not reduced in *AtMTP1* RNA interference transformants (Fig. 5B). Root elongation was significantly more sensitive to

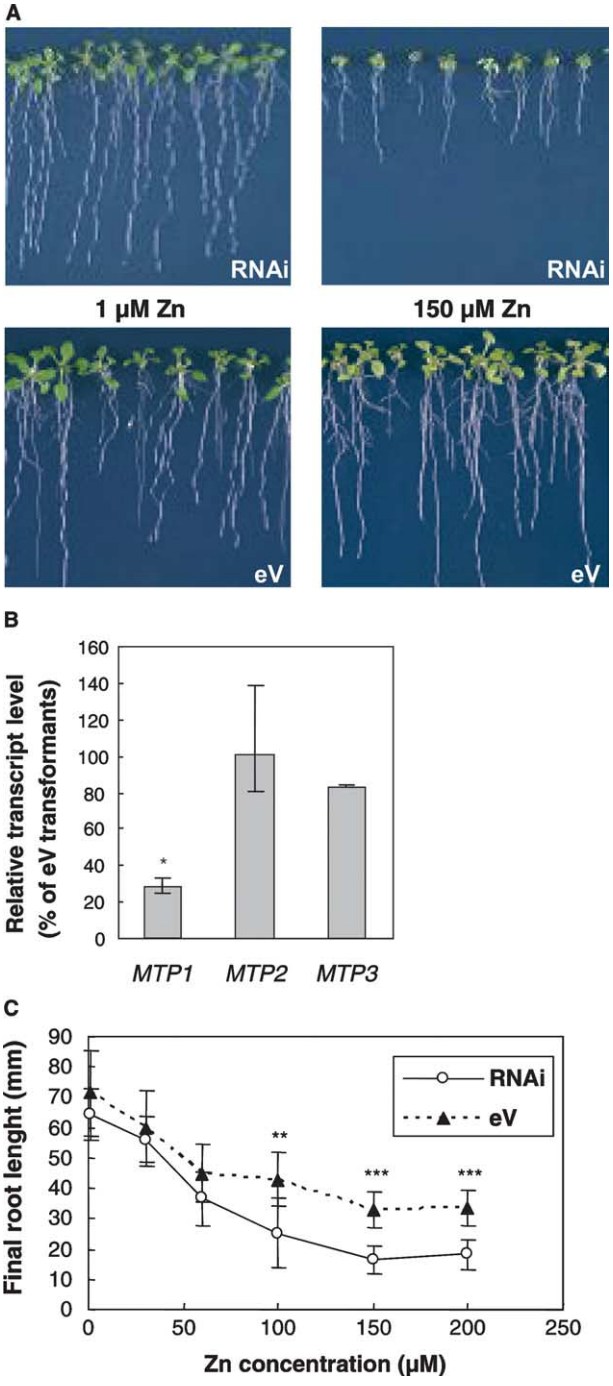

Fig. 5. Silencing of *AtMTP1* by RNA interference causes Zn hypersensitivity. (A) Photograph showing 17-day-old T1 individuals transformed with the *AtMTP1* RNA interference construct (top) or an empty vector (bottom) after growth on media containing normal (1 µM, left) or high (150 µM, right) concentrations of $ZnSO_4$. Note that each seedling of the T1 generation represents an independent transformant line. (B) Quantitative real-time RT-PCR analysis of *MTP1, MTP2* and *MTP3* transcript levels in *AtMTP1*-RNAi transformants. Values are average transcript levels in *AtMTP1* RNAi transformants normalized to empty vector transformants (arithmetic mean ± S.E. of $n = 3$ independent experiments). In each experiment, 4 seedlings of the T1 generation were pooled for analysis. For *AtMTP1*, ΔC_T values for RNAi plants were significantly different from those in empty vector controls ($P < 0.05$; Student's t test, with Bonferroni adjustments for multiple comparisons). (C) Final root length as a function of Zn concentration in the growth medium for *AtMTP1* RNAi and empty vector transformants as shown in (A). Values are arithmetic means ± S.D. of 20 replicate seedlings from one experiment representative of a total of three independent experiments. After selection of transformants, 10-day-old seedlings were transferred onto plates containing a modified Hoagland's medium and added $ZnSO_4$ as indicated, for 7 days. Asterisks indicate the level of significance of differences between empty vector and *MTP1*-RNAi transformant plants ($^{**}P < 0.01$; $^{***}P < 0.001$, Student's t test, with Bonferroni adjustments for multiple comparisons).

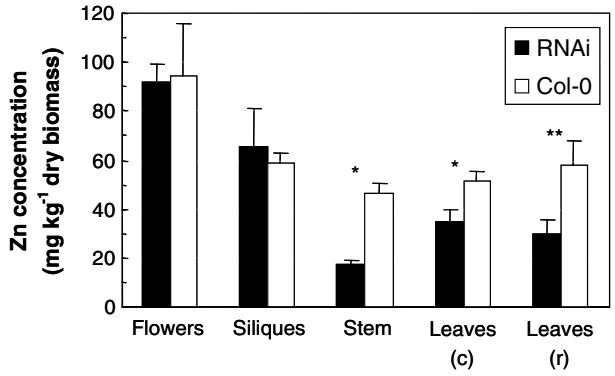

Fig. 6. Zn accumulation is decreased in *A. thaliana* transformed with an *AtMTP1* RNA interference construct. Each value is the arithmetic mean ± S.D. of zinc concentrations in three independent replicate samples, for each of which material was pooled from three individual plants of the T1 generation. Transformants were selected on plates as described in Fig. 5. Seventeen-day-old seedlings were transferred onto soil and grown for 27 days before harvest and analysis by ICP-OES. *A. thaliana* (Col) wild-type plants were used as controls. Data shown are from one experiment representative of a total of three independent experiments. Asterisks indicate the level of significance of differences between wild-type and transgenic plants ($^{*}P < 0.05$; $^{**}P < 0.01$; Student's *t* test).

Zn in *AtMTP1*-RNAi transformants than in empty vector transformants at 100, 150 and 200 μM Zn (Fig. 5C). There was no difference in root elongation under control (low zinc; Fig. 5C) or zinc deficiency conditions (data not shown). This suggests that MTP1 contributes to basal Zn tolerance in *A. thaliana*.

To investigate whether MTP1 contributes to Zn accumulation in *A. thaliana*, Zn concentrations were analyzed in various organs collected from mature plants grown on soil. Compared to the wild-type, Zn concentrations were significantly lower in the inflorescence stem (42% of wild-type) and in cauline leaves (68% of wild-type) and rosette leaves (50% of wild-type) of *AtMTP1* RNA interference plants (Fig. 6). Compared to empty vector transformants *MTP1* RNAi plants contained 80%, 91% and 65% Zn in the stem, in cauline leaves and rosette leaves, respectively, in an independent experiment (data not shown; $P < 0.05$, $P < 0.05$, $P < 0.001$ in a Student's *t* test, respectively). This suggests that AtMTP1 is involved in determining the strength of these organs as depositories for Zn in *A. thaliana*. In contrast, Zn concentrations in reproductive sink organs, namely flowers and siliques, which contained the highest Zn concentrations, appeared unaffected by reduced *AtMTP1* expression. In seeds of wild-type and RNAi plants, Zn concentrations were 46.7 ± 2.1 mg kg^{-1} ($n = 3$ independent replicates) and 39.2 ± 1.6 mg kg^{-1} ($n = 3$), respectively. It has to be kept in mind that the residual levels of *AtMTP1* transcript in the RNA interference plants imply that some MTP1 protein was likely to be present in these plants.

4. Discussion

Here we identify a mutation in AtMTP1, $AtMTP1_{D94A}$, the expression of which is unable to complement Zn sensitivity of the *zrc1 cot1* double mutant. We show that this mutation renders the yeast double mutant distinctly hypersensitive to Zn (Fig. 1). This observation suggests that $AtMTP1_{D94A}$ cannot transport Zn, and it is consistent with the hypothesis that the mutant transporter introduces an ion leak into the yeast vacuolar membrane. AtMTP1 localizes to the vacuolar membrane of plant cells when expressed transiently with an N-terminally fused GFP moiety, or stably with a C-terminally fused EGFP (Fig. 2). These data support the idea of a cellular function of MTP1 in Zn detoxification by transport of Zn across the vacuolar membrane into the vacuole for sequestration. The localization of AtMTP1 reported here is different from the localization of *T. goesingense* MTP1, which has been reported to localize to the plasma membrane [28]. MTP1 proteins from *A. halleri* [29] and poplar [24] have been reported to localize to the vacuolar membrane. Our results are in agreement with the localization of a transiently expressed AtMTP1-GFP fusion protein and the fractionation of AtMTP1 in a sucrose density gradient reported recently [31]. However, these authors could not detect a GFP signal when protoplasts were transiently transfected with a construct encoding GFP fused to the N-terminus of the MTP1 protein. *A. thaliana* NRAMP3 (natural resistance-associated macrophage protein 3), a member of a distinct family of transition metal transport proteins, was also localized to the vacuolar membrane and was proposed to have a role in the release of transition metals, including iron, from vacuoles [47].

In oocytes, expression of AtMTP1 confers the ability to accumulate Zn (Table 1). By contrast, expression of $AtMTP1_{D94A}$ does not confer Zn accumulation to oocytes, consistent with the results in yeast, which suggested that $AtMTP1_{D94A}$ is unable to transport Zn. The accumulation of Zn in oocytes expressing AtMTP1 suggests that in this expression system, a proportion of the transporter localizes to the plasma membrane. Localization of functionally significant amounts of heterologously expressed plant tonoplast proteins to the plasma membrane of *Xenopus* oocytes has been reported for other proteins [35] and is likely to be a consequence of the high expression levels and the absence of a large central vacuole in oocytes. In plant cells, AtMTP1 generally mediates the export of Zn from the cytoplasm. Oocytes injected with *MTP1* cRNA and incubated under low-Zn (0 Zn) conditions contained lower Zn concentrations than water-injected or $MTP1_{D94A}$-injected oocytes. This may reflect MTP1-mediated efflux of Zn contained in the oocytes during incubation in media lacking added Zn between cRNA injection and harvest. Our data strongly suggest that the direction of MTP1-mediated Zn transport can be reversed under conditions of high external Zn^{2+} in the oocyte expression system. It may therefore be feasible to analyze MTP1 transport properties in oocytes using electrophysiological techniques.

Real-time RT-PCR analysis of bulk tissues from different organs of *A. thaliana* indicate a widespread and uniform expression of the *AtMTP1* transcript (Fig. 3). An analysis of lines transformed with a promoter-reporter gene construct suggests that the rate of synthesis and translation of the spliced *AtMTP1* mRNA is particularly high during very young growth stages of the plant, as well as in growing tissues of *A. thaliana* plants at all ages (Fig. 4). Silencing of *AtMTP1* in *A. thaliana* by RNA interference causes hypersensitivity of root elongation to excess Zn, suggesting that AtMTP1 contributes to basal Zn tolerance in *A. thaliana* (Fig. 5). Dividing and elongating cells may be particularly sensitive to Zn toxicity. It is conceivable that damage to cells in the growing region of a plant directly inhibits growth. A constitutively high abundance of *MTP1*-re-

lated transcripts has recently been implicated in naturally selected Zn hypertolerance in the Zn hyperaccumulator plant *A. halleri* [29]. This may reflect higher *MTP1* transcript levels or a more widespread localization of *MTP1* expression in *A. halleri*, when compared to *A. thaliana* (see Fig. 4).

Recently, Zn hypersensitivity has also been reported in the *A. thaliana mtp1-1* T-DNA insertion line [31]. A significant difference between root elongation in wild-type and *mtp1-1* seedlings was apparent at a concentration of 400 μM Zn on MS agar plates [31]. Root elongation of *MTP1*-RNAi plants was significantly lower than in wild-type plants at Zn concentrations of 100 μM Zn and above (Fig. 5C). The iron concentrations was much lower in the medium used here than in the MS medium used by Kobae et al. [31] (5 μM FeHBED in Hoagland solution vs. 100 μM FeEDTA in MS medium). It is known that the addition of extra iron reduces metal toxicity [48]. We did not detect an increase in *MTP1* transcript levels in plants exposed to an excess of Cd, Co, Cu, Fe or Mn for 2 days (data not shown). Heterologous expression of MTP1 in yeast cells does not confer tolerance to Cd, Mn or Fe and confers only very low levels of Co tolerance (A.-G. Desbrosses-Fonrouge and U. Krämer, unpublished data). Earlier reports suggested that purified MTP1 protein reconstituted into proteoliposomes is able to transport Zn^{2+}, but not Cd^{2+} or Co^{2+} [49]. In agreement with this, root elongation in the *mtp1-1* mutant was equivalent to wild-type plants following exposure to 80 μM Co, 40 μM Ni, 1.5 mM Mn or 40 μM Cd in MS agarose medium [31]. Thus, all available data suggest that the function of MTP1 is Zn-specific.

Despite the specific function of the MTP1 protein in Zn detoxification by sequestration in the cell vacuole, *MTP1* transcript levels are not upregulated in response to exposure to excess Zn or Zn deficiency in the culture medium [25,29,50]. In agreement with this, there was no Zn-induced increase in MTP1 protein levels in a suspension culture derived from roots of *A. thaliana* [31]. Compared to the root-derived suspension culture, MTP1 protein levels were very low in a suspension culture derived from whole *A. thaliana* seedlings. The authors suggested that the MTP1 protein content of the suspension cultures may reflect the MTP1 protein content in the cell type or tissue of origin. Our results provide experimental support for the hypothesis that MTP1 expression is localized to specific cell types in *A. thaliana* plants.

The silencing of *AtMTP1* also results in a reduction in Zn concentrations in rosette and cauline leaves and in the inflorescence stem (Fig. 6). Thus, in vegetative tissues, *MTP1* expression is necessary for the accumulation of normal concentrations of Zn (Fig. 6). Kobae et al. [31] did not report Zn concentrations accumulated in the *mtp1-1* mutant. Based on the localization of the MTP1 protein in the vacuolar membrane, a model can be envisaged, in which the rate of MTP1-mediated vacuolar sequestration drives the rate of cellular Zn uptake, the delivery of Zn to the respective tissue via long distance transport in the plant and possibly also root Zn uptake. This raises the question of whether a localized ectopic expression of MTP1 is sufficient to increase the accumulation of Zn in the respective cells. Zinc hyperaccumulator plants such as *A. halleri* are known to accumulate Zn specifically in their leaf biomass. It will be very interesting to investigate whether *A. halleri MTP1* genes are not only important for Zn tolerance [29], but also play a role in leaf zinc accumulation.

In *Arabidopsis* plants exhibiting *MTP1* silencing by RNA interference a decrease in Zn accumulation was less pronounced or absent in flowers, siliques and seeds. It is likely that in these tissues MTP1 is functionally redundant. This idea is supported by AtGenExpress data, which suggest that transcripts encoding other MTP1-related transporters, namely MTP2 and MTP4, as well as MTP3 (our own unpublished data) are present in floral organs and in developing seeds. A further possibility could be that in these tissues Zn accumulation is primarily driven by zinc delivery rather than by Zn sequestration.

AtMTP1 promoter activity was primarily detected in growing regions of the plant. In *A. thaliana* plants, in which *MTP1* was silenced by RNA interference, Zn concentrations were lower than in wild-type plants in bulk leaves and stems. To conciliate these results, two hypotheses could be tested. The MTP1 protein could be stable so that it is synthesized in young leaves but still present in older leaves. Alternatively, MTP1-driven Zn accumulation in a leaf may occur at a young stage, with sequestration in the vacuole at least partly driving total cellular Zn accumulation, and total leaf Zn content may be largely maintained in mature leaves.

In summary, we provide evidence at the cellular and whole-plant level to support that AtMTP1 is a Zn transporter localized in the vacuolar membrane and mediates Zn detoxification and storage by vacuolar sequestration of Zn. Our data suggest that the primary role of MTP1 is to contribute to cellular metal accumulation and to basal metal tolerance in cells of growing tissues.

Acknowledgements: This work was supported by a joint PROCOPE travel Grant (D/0122934) awarded to S.T. and U.K. by the German Academic Exchange Service. Further support was provided by the EU research training network METALHOME (HPRN-CT-2002-00243, S.T., U.K.), by the EU RTD project METALLOPHYTES (QLK3-2000-00479, A.-G. D.-F., U.K.), by the Deutsche Forschungsgemeinschaft (Arabidopsis Functional Genomics Network AFGN, Kr 1967/2-1 and 2-2, S.A. and U.K.), and by the German Federal Ministry of Education and Research (Biofuture Grant 0311877, K.V., A.S. and U.K.).

References

[1] Clarke, N.D. and Berg, J.M. (1998) Zinc fingers in *Caenorhabditis elegans*: finding families and probing pathways. Science 282, 2018–2022.
[2] Coleman, J.E. (1998) Zinc enzymes. Curr. Opin. Chem. Biol. 2, 222–234.
[3] Hambidge, M. (2000) Human zinc deficiency. J. Nutr. 130, 1344S–1349S.
[4] Wang, K., Zhou, B., Kuo, Y.M., Zemansky, J. and Gitschier, J. (2002) A novel member of a zinc transporter family is defective in *Acrodermatitis enteropathica*. Am. J. Hum. Genet. 71, 66–73.
[5] Kury, S., Dreno, B., Bezieau, S., Giraudet, S., Kharfi, M., Kamoun, R. and Moisan, J.P. (2002) Identification of SLC39A4, a gene involved in *Acrodermatitis enteropathica*. Nat. Genet. 31, 239–240.
[6] Woolhouse, H.W. (1983) (Lange, O.L., Nobel, P.S., Osmond, C.B. and Ziegler, H., Eds.), Encyclopedia of Plant Physiology: Responses to the Chemical and Biological Environment, Vol. sNew Series Vol. 12 C, Springer Verlag, Berlin.
[7] Zhao, H. and Eide, D. (1996) The yeast *ZRT1* gene encodes the zinc transporter protein of a high-affinity uptake system induced by zinc limitation. Proc. Natl. Acad. Sci. USA 93, 2454–2458.
[8] Zhao, H. and Eide, D. (1996) The *ZRT2* gene encodes the low affinity zinc transporter in *Saccharomyces cerevisiae*. J. Biol. Chem. 271, 23203–23210.

[9] Grotz, N., Fox, T., Connolly, E., Park, W., Guerinot, M.L. and Eide, D. (1998) Identification of a family of zinc transporter genes from *Arabidopsis* that respond to zinc deficiency. Proc. Natl. Acad. Sci. USA 95, 7220–7224.
[10] Gaither, L.A. and Eide, D.J. (2000) Functional expression of the human hZIP2 zinc transporter. J. Biol. Chem. 275, 5560–5564.
[11] Wang, F., Dufner-Beattie, J., Kim, B.E., Petris, M.J., Andrews, G. and Eide, D.J. (2004) Zinc-stimulated endocytosis controls activity of the mouse ZIP1 and ZIP3 zinc uptake transporters. J. Biol. Chem. 279, 24631–24639.
[12] Kim, B.E., Wang, F., Dufner-Beattie, J., Andrews, G.K., Eide, D.J. and Petris, M.J. (2003) Zn^{2+}-stimulated endocytosis of the mZIP4 zinc transporter regulates its location at the plasma membrane. J. Biol. Chem. 279, 4523–4530.
[13] Gitan, R.S., Luo, H., Rodgers, J., Broderius, M. and Eide, D.J. (1998) Zinc-induced inactivation of the yeast ZRT1 zinc transporter occurs through endocytosis and vacuolar degradation. J. Biol. Chem. 273, 28617–28624.
[14] MacDiarmid, C.W., Milanick, M.A. and Eide, D.J. (2003) Induction of the *ZRC1* metal tolerance gene in zinc-limited yeast confers resistance to zinc shock. J. Biol. Chem. 278, 15065–15072.
[15] MacDiarmid, C.W., Gaither, A.L. and Eide, D. (2000) Zinc transporters that regulate vacuolar zinc storage in *Saccharomyces cerevisiae*. EMBO J. 19, 2845–2855.
[16] Kamizono, A., Nishizawa, M., Teranishi, Y., Murata, K. and Kimura, A. (1989) Identification of a gene conferring resistance to zinc and cadmium ions in the yeast *Saccharomyces cerevisiae*. Mol. Gen. Genet. 219, 161–167.
[17] Conklin, D.S., McMaster, J.A., Culbertson, M.R. and Kung, C. (1992) *COT1*, a gene involved in cobalt accumulation in *Saccharomyces cerevisiae*. Mol. Cell. Biol. 12, 3678–3688.
[18] Gaither, L.A. and Eide, D.J. (2001) Eukaryotic zinc transporters and their regulation. Biometals 14, 251–270.
[19] MacDiarmid, C.W., Milanick, M.A. and Eide, D.J. (2002) Biochemical properties of vacuolar zinc transport systems of *Saccharomyces cerevisiae*. J. Biol. Chem. 277, 39187–39194.
[20] Guffanti, A.A., Wei, Y., Rood, S.V. and Krulwich, T.A. (2002) An antiport mechanism for a member of the cation diffusion facilitator family: divalent cations efflux in exchange for K^+ and H^+. Mol. Microbiol. 45, 145–153.
[21] Chao, Y. and Fu, D. (2004) Kinetic study of the antiport mechanism of an *Escherichia coli* zinc transporter ZitB. J. Biol. Chem. 279, 12043–12050.
[22] Palmiter, R.D. and Huang, L. (2004) Efflux and compartmentalization of zinc by members of the SLC30 family of solute carriers. Pflugers Arch. 447, 744–751.
[23] Paulsen, I.T. and Saier Jr., M.H. (1997) A novel family of ubiquitous heavy metal ion transport proteins. J. Membr. Biol. 156, 99–103.
[24] Blaudez, D., Kohler, A., Martin, F., Sanders, D. and Chalot, M. (2003) Poplar metal tolerance protein 1 (MTP1) confers zinc tolerance and is an oligomeric vacuolar zinc transporter with an essential leucine zipper motif. Plant Cell 15, 2911–2928.
[25] Van der Zaal, B.J., Neuteboom, L.W., Pinas, J.E., Chardonnens, A.N., Schat, H., Verkleij, J.A.C. and Hooykaas, P.J.J. (1999) Overexpression of a novel *Arabidopsis* gene related to putative zinc-transporter genes from animals can lead to enhanced zinc resistance and accumulation. Plant Physiol. 119, 1047–1055.
[26] Mäser, P. et al. (2001) Phylogenetic relationships within cation transporter families of *Arabidopsis*. Plant Physiol. 126, 1646–1667.
[27] Persans, M.W., Nieman, K. and Salt, D.E. (2001) Functional activity and role of cation-efflux family members in Ni hyperaccumulation in *Thlaspi goesingense*. Proc. Natl. Acad. Sci. USA 98, 9995–10000.
[28] Kim, D., Gustin, J.L., Lahner, B., Persans, M.W., Baek, D., Yun, D.J. and Salt, D.E. (2004) The plant CDF family member TgMTP1 from the Ni/Zn hyperaccumulator *Thlaspi goesingense* acts to enhance efflux of Zn at the plasma membrane when expressed in *Saccharomyces cerevisiae*. Plant J. 39, 237–251.
[29] Dräger, D.B., Desbrosses-Fonrouge, A.G., Krach, C., Chardonnens, A.N., Meyer, R.C., Saumitou-Laprade, P. and Krämer, U. (2004) Two genes encoding *Arabidopsis halleri* MTP1 metal transport proteins co-segregate with zinc tolerance and account for high *MTP1* transcript levels. Plant J. 39, 425–439.
[30] Delhaize, E., Kataoka, T., Hebb, D.M., White, R.G. and Ryan, P.R. (2003) Genes encoding proteins of the cation diffusion facilitator family that confer manganese tolerance. Plant Cell 15, 1131–1142.
[31] Kobae, Y., Uemura, T., Sato, M.H., Ohnishi, M., Mimura, T., Nakagawa, T. and Maeshima, M. (2004) Zinc transporter of *Arabidopsis thaliana* AtMTP1 is localized to vacuolar membranes and implicated in zinc homeostasis. Plant Cell Physiol. 45, 1749–1758.
[32] Becher, M., Talke, I.N., Krall, L. and Krämer, U. (2004) Cross-species microarray transcript profiling reveals high constitutive expression of metal homeostasis genes in shoots of the zinc hyperaccumulator *Arabidopsis halleri*. Plant J. 37, 251–268.
[33] Sambrook, J. and Russel, D.W. (2001) Cold Spring Harbor Laboratory Press, Cold Spring Harbor, New York.
[34] Liman, E.R., Tytgat, J. and Hess, P. (1992) Subunit stoichiometry of a mammalian K^+ channel determined by construction of multimeric cDNAs. Neuron 9, 861–871.
[35] Maurel, C., Reizer, J., Schroeder, J.I. and Chrispeels, M.J. (1993) The vacuolar membrane protein gamma-TIP creates water specific channels in *Xenopus* oocytes. EMBO J. 12, 2241–2247.
[36] Lämmli, U.K. (1970) Cleavage of structural proteins during the assembly of the head of bacteriophage T4. Nature 227, 680–685.
[37] Towbin, H., Staehelin, T. and Gordon, J. (1979) Electrophoretic transfer of proteins from polyacrylamide gels to nitrocellulose sheets: procedure and some applications. Proc. Natl. Acad. Sci. USA 46, 4350–4354.
[38] Davis, S.J. and Vierstra, R.D. (1998) Soluble, highly fluorescent variants of green fluorescent protein (GFP) for use in higher plants. Plant Mol. Biol. 36, 521–528.
[39] Haseloff, J., Siemering, K.R., Prasher, D.C. and Hodge, S. (1997) Removal of a cryptic intron and subcellular localization of green fluorescent protein are required to mark transgenic *Arabidopsis* plants brightly. Proc. Natl. Acad. Sci. USA 94, 2122–2127.
[40] Karimi, M., Inze, D. and Depicker, A. (2002) GATEWAY vectors for *Agrobacterium*-mediated plant transformation. Trends Plant Sci. 7, 193–195.
[41] Clough, S.J. and Bent, A.F. (1998) Floral dip: a simplified method for Agrobacterium-mediated transformation of *Arabidopsis thaliana*. Plant J. 16, 735–743.
[42] Czechowski, T., Bari, R.P., Stitt, M., Scheible, W.R. and Udvardi, M.K. (2004) Real-time RT-PCR profiling of over 1400 Arabidopsis transcription factors: unprecedented sensitivity reveals novel root- and shoot-specific genes. Plant J. 38, 366–379.
[43] Ramakers, C., Ruijter, J.M., Deprez, R.H. and Moorman, A.F. (2003) Assumption-free analysis of quantitative real-time polymerase chain reaction (PCR) data. Neurosci. Lett. 339, 62–66.
[44] Becker, D. (1990) Binary vectors which allow the exchange of plant selectable markers and reporter genes. Nucleic Acids Res. 18, 203.
[45] Falchuk, K.H. and Montorzi, M. (2001) Zinc physiology and biochemistry in oocytes and embryos. Biometals 14, 385–395.
[46] Helliwell, C. and Waterhouse, P. (2003) Constructs and methods for high-throughput gene silencing in plants. Methods 30, 289–295.
[47] Thomine, S., Lelievre, F., Debarbieux, E., Schroeder, J.I. and Barbier-Brygoo, H. (2003) AtNRAMP3, a multispecific vacuolar metal transporter involved in plant responses to iron deficiency. Plant J. 34, 685–695.
[48] Wycisk, K., Kim, E.J., Schroeder, J.I. and Krämer, U. (2004) Enhancing the first enzymatic step in the histidine biosynthesis pathway increases the free histidine pool and nickel tolerance in *Arabidopsis thaliana*. FEBS Lett. 578, 128–134.
[49] Bloss, T., Clemens, S. and Nies, D.H. (2002) Characterization of the ZAT1p zinc transporter from *Arabidopsis thaliana* in microbial model organisms and reconstituted proteoliposomes. Planta 214, 783–791.
[50] Wintz, H., Fox, T., Wu, Y.Y., Feng, V., Chen, W., Chang, H.S., Zhu, T. and Vulpe, C. (2003) Expression profiles of *Arabidopsis thaliana* in mineral deficiencies reveal novel transporters involved in metal homeostasis. J. Biol. Chem. 278, 47644–47653.